

# Nanostructured Metal-Organic Composite Solar Cells

## Investigators

Mark L. Brongersma, Associate Professor, Materials Science and Engineering; Shanhui Fan, Associate Professor, Electrical Engineering; Peter Peumans, Assistant Professor, Electrical Engineering; Peter Catrysse, Post-doctoral researcher; Ed Bernard and Jung-Yong Lee Graduate Researchers, Visiting scholar: Shigeo Fujimori, PhD.

## Abstract

This project was aimed at realizing a high efficiency organic photovoltaic (PV) device using nanoscale metallic features to enhance the overall cell performance. The goals of the project were threefold. The first aim was to develop transparent high-sheet-conductivity nanopatterned metal films for use as transparent conductors that allow more light to enter a PV cell and enable parallel subcell connection. The second goal was to develop novel synthesis routes for metallic nanostructures that strongly interact with light and can effectively concentrate or trap light in a PV cell. The third and final goal was to embed these nanostructures in the active layers of an organic solar cell and determine the enhancements in the photon absorption and charge separation efficiency.

Our strategy to generate transparent metallic contacts was based on introducing arrays of deep-subwavelength holes into them. In full-field electromagnetic simulations, we found that sub-wavelength cylindrical holes in a metal always support a propagating mode near its surface plasmon frequency, regardless of how small the holes are. This is very different from the microwave regime where the metal behaves as perfect electrical conductors. The propagating (HE<sub>11</sub>) mode is located completely below the surface plasmon frequency (in the UV part of the spectrum) and gives rise to a pass-band in the transmission spectrum. We subsequently discovered that by concentrically filling nanoscale holes with dielectric materials, it was possible to generate a very wide passband of many hundreds of nanometer. In order to help engineers in the design of such holes, we made an explicit connection between the dispersion of coaxial plasmonic structures that support deep-subwavelength propagating modes, and the planar metal-insulator-metal geometry. The latter geometry is well-known from the current literature and provides intuitive an intuitive vantage point from which the more complex cylindrical structures can be understood and optimized.

The second major area was the synthesis and optical characterization of metallic nanostructures that can be incorporated in the organic solar cells. One way by which we have synthesized metallic nanowire structures is by electrochemical means into porous materials, such as nanoporous anodized alumina or ion track-etched polycarbonate (PC) membranes. Using this method, we generated gold, silver, and gold/silver heterostructure nanowires with diameters in the range from 30 nm – 50 nm and lengths ranging from 100 nm – 1  $\mu$ m. The strong light scattering from these wires was confirmed in a homebuilt dark-field light scattering setup and the scattering properties were analyzed spectrally and compared to analytic Mie theory. We also synthesized 10 nm diameter Ag nanoparticles with 3 nm thick SiO<sub>2</sub> coatings in solution. These particles were incorporated into organic thin films and their effect on the luminescence and optical

absorption was analyzed. We found that, despite the 3 nm thick SiO<sub>2</sub> coating, the Ag nanoparticles still had a very strong enhancing effect on the optical absorption and that this enhancement was broadband.

We have also generated simple engineering models for the design of the optimum metallic nanostructures for light trapping and concentration. We found that metallic antennas can simply be described as Fabry-Perot cavities for surface plasmon-polariton waves. For this reason, such structures enable a very strong light-matter interaction when the metal antenna length equals about half a surface plasmon-polariton wavelength, which can be substantially shorter than the free space wavelength of light. This notion enables a better design of the antennas that can be incorporated into organic solar cells to enable enhancements in light absorption near a donor\acceptor interface.

As the third major research direction in our team effort, we aimed to include the solution-synthesized metal nanoparticles into an organic solar cell without exposing the organic materials to solvents. The basic method was developed earlier under Peumans' Molecular Solar Cells GCEP grant for the inclusion of inorganic structures into organic solar cells. This method was then applied to include gold nanoparticles and nanorods at the active interface of simple bilayer organic solar cells, leading to an enhancement of their efficiency. We experimentally demonstrated increases in photocurrent by 20% to 30% related to the incorporation of metallic nanostructures. These enhancements were in agreement with full-field electromagnetic simulations.

Finally, we have used a very general theoretical framework to determine the maximum optical absorption in a limited volume of absorbing medium; Achieving the highest possible optical absorption for a given volume or thickness of an absorber is a general and very important problem in solar cells. The amount of active material (absorber) used is minimized to either minimize cost (in crystalline Silicon) or to maximize the internal efficiency (all solar cells and organic solar cells in particular). Several approaches have been developed, such as textures, gratings (guided resonances), cavities, plasmonic approaches, optical antennas, etc. The derivation was based on concepts borrowed from information theory (singular value decomposition) and showed that the limit is identical to that derived earlier for the geometric optics regime.

## **Introduction**

Organic-based solar cells have high potential to reduce the cost of photovoltaics. Low-cost active materials, high-throughput reel-to-reel deposition technologies, and application versatility makes them very likely to become competitive against inorganic thin-film devices. However the power conversion efficiency of organic photovoltaics (OPV) is still too low. This project aims at realizing a high efficiency organic devices by exploiting the unique optical properties of metal to realize high-sheet-conductivity and virtually transparent contacts. It also aims at optimizing the use of metal nanostructures in the active layers to enhance the photon absorption and charge separation efficiency.

## Background

The performance of organic photovoltaics has been improving relatively quickly in the last few years. However this technology is still facing major fundamental limitations towards higher efficiency and stability that need to be overcome for it to be competitive with inorganic thin-film solar cells. This project proposes an innovative cell design to increase the efficiency of organic photovoltaics: a stack of organic/inorganic heterojunctions with embedded nanostructured metal features to improve the overall cell performance. The stack design is a high potential route to increase the light absorption efficiency of photovoltaics. The splitting of the solar spectrum through complementary absorption by different cells with specifically designed bandgaps minimizes thermal losses and increases the overall photon conversion efficiency.

## Results

During the three year of the project progress has been made in several research directions outlined below. One key area of research was the design of transparent metallic contacts that contain engineered subwavelength hole arrays. In the process, we realized deep-subwavelength apertures in thin metal films that support propagating plasmonic modes that cover the entire solar spectrum. For sub-wavelength apertures in metallic films, it is well known that the transmission characteristics are strongly influenced by the presence or absence of propagating optical modes inside the apertures. For cylindrical holes with a circular cross section, the prevailing wisdom dictates that they do not support propagating modes when the hole diameter is much smaller than  $\lambda/2n_0$ , where  $\lambda$  is the vacuum wavelength of incident light and  $n_0$  is the refractive index of the dielectric filling the hole. Nevertheless, sub-wavelength cylindrical holes in a plasmonic metal, in fact, always support a propagating mode near the surface plasmon frequency, regardless of how small the holes are. This is very different from the microwave regime where the metal behaves as perfect electrical conductors. The propagating  $HE_{11}$  mode is located completely below the surface plasmon frequency and gives rise to a pass-band in the transmission spectrum. However, the bandwidth of the  $HE_{11}$  mode asymptotically approaches zero as hole size is reduced to zero. Thus such a mode may not play a prominent role as the hole size becomes far smaller than the wavelength of the incident light.

With the support of the GCEP program, we discovered that by concentrically filling nano-scale holes with two different dielectric materials, it is possible to significantly extend the bandwidth of the  $HE_{11}$  mode. By dispersion relation analysis, we show that using this approach it is possible to create nano-scale propagating modes with very large bandwidth even when the hole radius goes to zero. (Figure 1)

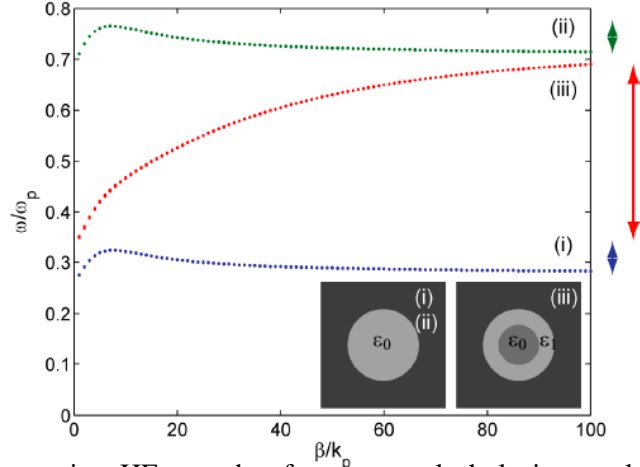


**Figure 1:** Propagating  $\text{HE}_{11}$  mode of a nano-scale hole in metal with plasma wavelength  $\lambda_p$ . (e.g. or silver  $\lambda_p = 138\text{nm}$ ). Dispersion diagram for (i) low-index core (Green curve,  $r_0 = 0.036$ ,  $\lambda_p = 5\text{nm}$ ,  $\epsilon_0 = 1$ ). (ii) High index core. (Blue curve,  $r_0 = 0.036$ ,  $\lambda_p = 5\text{nm}$ ,  $\epsilon_0 = 12$ ). (iii) Dielectric core with concentric rings of high and low indices. (Red curve.)

The structure we consider is shown in the inset (iii) of Fig. 1 and represents a  $z$ -invariant waveguide with a cylindrical cross-section in the transverse  $xy$ -plane with an external radius  $r_m$ . Inside the waveguide, we assume two concentric dielectric regions: a central disk with radius  $r_1$  and a concentric ring of width  $r_m - r_1$ . For the dielectric materials inside these regions, we use real frequency-independent dielectric constants  $\epsilon_1$  and  $\epsilon_2$ . For the surrounding metal, we use a complex frequency-dependent model:

$$\epsilon_m(\omega) = 1 - \frac{\omega_p^2}{\omega(\omega - i\omega_\tau)}, \quad (1)$$

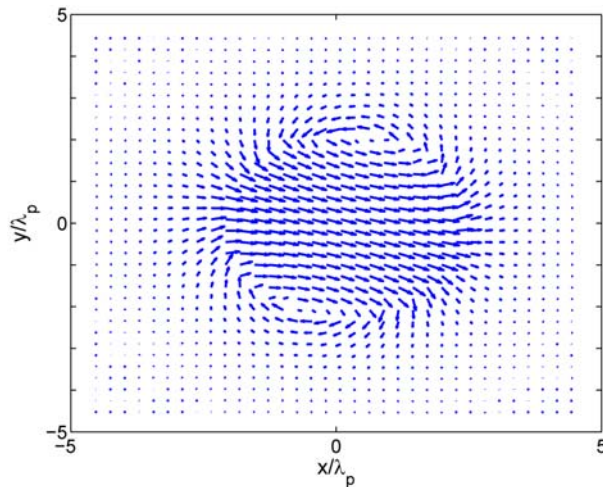
where  $\omega_p$  is the plasma frequency and  $\omega_\tau$  is the collision frequency. We derive and solve a transcendental equation to calculate the dispersion relation  $(\beta, \omega)$  of propagating modes inside a cylindrical hole, where  $\beta$  is the propagation vector along the  $z$ -axis of the waveguide and  $\omega$  is the radial frequency.

In general, sub-wavelength holes in a plasmonic metal always support a fundamental  $\text{HE}_{11}$  mode that is spectrally defined between an upper and a lower frequency limit. The upper limit occurs for  $\beta \rightarrow \infty$  and asymptotically approaches the surface plasmon frequency  $\omega_{sp} = \omega_p / \sqrt{\epsilon_0 + 1}$  of the metal-dielectric interface inside the hole, where  $\epsilon_0$  is the dielectric constant of the dielectric near the interface. In this limit, the mode is tightly confined to the metal-dielectric interface and senses the dielectric and metal in its immediate vicinity only. The lower limit occurs when  $\beta = 0$  and represents the cutoff

frequency  $\omega_c$  of the  $\text{HE}_{11}$  mode. For holes filled with a uniform dielectric, the limiting frequencies are intrinsically coupled through the dielectric constant of the uniform material inside the hole. As a result, the cutoff frequency  $\omega_c$  of the  $\text{HE}_{11}$  mode asymptotically approaches surface plasmon frequency  $\omega_{sp}$  and the bandwidth of the mode,  $\omega_{sp} - \omega_c$  goes to zero when hole size is reduced to deep sub-wavelength scale, which is required for many transparent electrode applications.

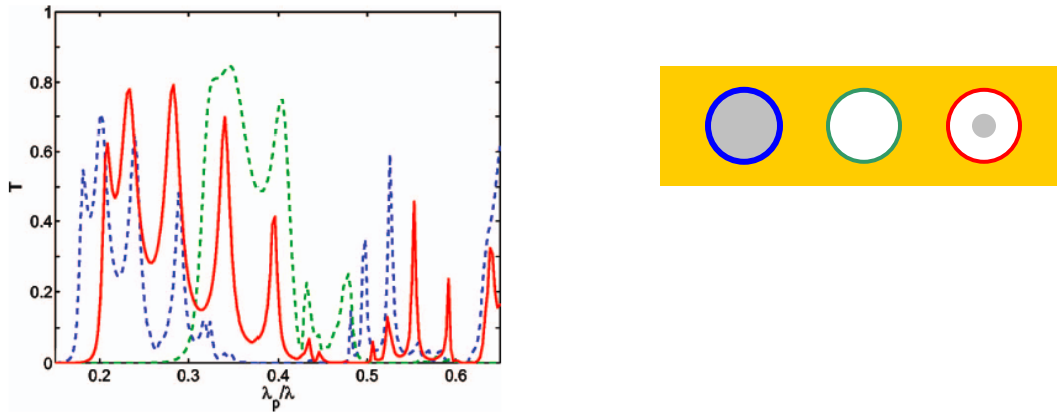
The observation that  $\omega_{sp}$  depends on the dielectric properties in the immediate vicinity of the interface only, while  $\omega_c$  depends on the dielectric properties across the entire hole, however, provides a possible mechanism for decoupling the limiting frequencies of the  $\text{HE}_{11}$  mode through the use of concentric dielectric rings. By effectively decoupling the dependence of the cut-off frequency ( $\beta = 0$ ) from that of the large- $\beta$  frequency, it is possible to engineer the behavior of both frequency limits (for  $\beta = 0$  and  $\beta \rightarrow \infty$ ) independently. This in turn enables complete control over the mode bandwidth. We note that in order to extend bandwidth, the cut-off frequency has to be lowered and the upper-frequency limit has to be raised. This is achieved by appropriate choice of dielectrics, i.e., the center region has to have a larger index and the concentric ring a lower index. (Figure 1)

Figure 2 shows a vector plot of the electric (displacement) field for the fundamental  $\text{HE}_{11}$  mode in a sub-wavelength hole filled with two concentric dielectric regions. The field orientation provides evidence that the propagating mode indeed has the proper symmetry for efficient coupling. Similarly, we have examined the fields of the next-higher-order  $\text{EH}_{11}$  mode (not shown here) and confirmed that it couples to normally incident light as well. This field analysis confirms the usefulness of these propagating modes in transporting of light collected/emitted at the entrance/exit of a sub-wavelength aperture.



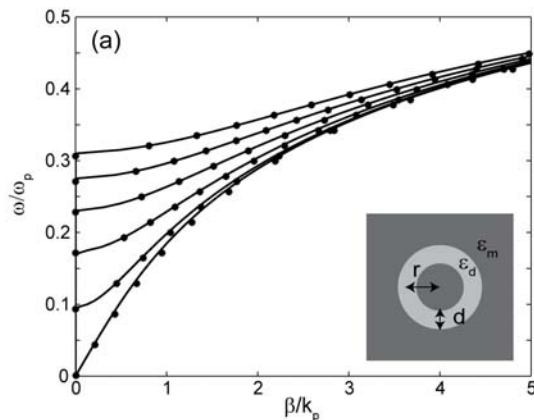
**Figure 2:** Electric field distributions for the propagating  $\text{HE}_{11}$  mode in a subwavelength cylindrical hole in metal. The dipolar field indicates that the mode will couple to external plane waves.

Figure 3 below shows optimized transmission spectra for three different apertures. As can be seen, the use of a dielectric rod at the center of aperture significantly broadens the transmission spectrum. Assuming a plasmonic wavelength of 200 nm, the improved design has a pass band that extends from infrared to the visible wavelength range, making them suitable for solar applications.



**Figure 3:** Transmission spectra for three different apertures shown in the inset. The green line is for an aperture with air inside. The blue line is for an aperture filled with dielectric. And the red line is for an aperture with a dielectric rod at the center. Notice that the structure with a dielectric rod in the center results in significant broadening of the passband of the structure.

As a final important feat, we made an explicit connection between the dispersion of coaxial plasmonic structures that support deep-subwavelength propagating modes, and the planar metal-insulator-metal geometry. With our approach, we provide an intuitive picture that allows to qualitatively understand and to quantitatively predict the entire dispersion behavior (Fig. 4), including the number of modes at every frequency, the modal propagation constants, the propagation losses, and the cut-off frequencies of propagating modes supported by a technologically important structure.



**Figure 4:** Dispersion relation of propagating modes supported by a structure with coaxial cross-section for a plasmonic metal. The curves are obtained from the analytical expression (solid lines) and from a numerical finite-difference frequency-domain method (filled circles).

The second major area was the synthesis and optical characterization of metallic nanostructures that can be incorporated in the organic solar cells. One way by which we have synthesized metallic nanowire structures is by electrochemical means into porous materials, such as nanoporous anodized alumina or ion track-etched polycarbonate (PC) membranes. As an example, Fig. 5(a) and (b) show scanning electron microscopy images of a bed of 30 nm diameter Ag nanowires and a close-up of a single Ag nanowire. To grow these particular wires, PC membranes were first coated with a seed layer of gold on the backside using a metal evaporator. These coated membranes were then immersed in an electroless silver-plating bath. The gold acted as a catalyst for silver precipitation and wires nucleated at the bottom of the pores. Growth continued as the silver was reduced from solution onto the silver precipitates. The porous membrane restricted the growth in one dimension. When wires reached their desired length, the membrane containing the wires was removed from solution and rinsed to remove residual plating solution. The nanowires were finally released into solution by dissolving away the porous membrane in chloroform and spun onto a glass substrate for further analysis. Using this technique large numbers of wires can be generated in an inexpensive fashion. These nanowires act as optical nano-antennas that can concentrate electromagnetic energy into a nanoscale volume. Dark-field optical microscopy studies were performed on these wires and resonantly enhanced light scattering was observed in the visible part of the electromagnetic spectrum. Figure 5(c) shows a representative dark-field optical microscopy of an Ag nanowire. By embedding such structures in OPV devices an improved light absorption, charge separation, and charge collection can be obtained. For example, when placed at the donor-acceptor interface of an organic heterojunction, electrically isolated metal nanoparticles may enhance photon absorption by concentrating the electromagnetic energy of incident radiation close to the junction.

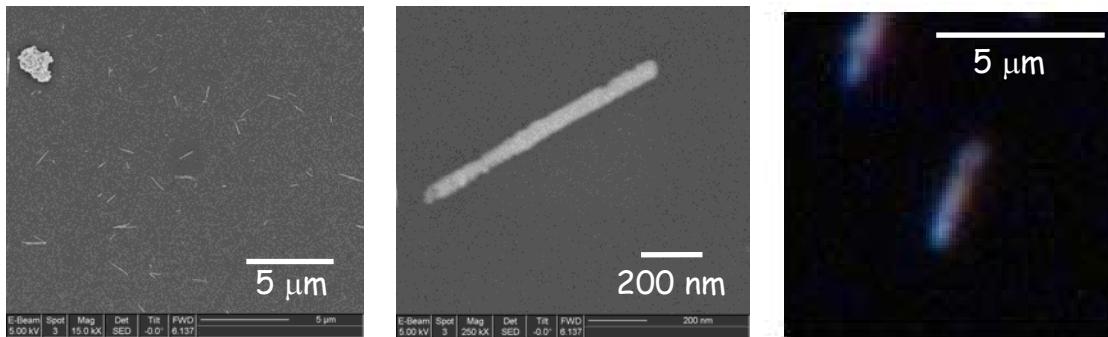


**Figure 5:** (a) Scanning electron microscopy (SEM) image of a bed of 30nm diameter Ag nanowires generated by electroless plating of Ag into a porous polycarbonate membrane. (b) SEM micrograph of a single Ag nanowire. (c) Dark-field optical microscopy image of a 30 nm diameter Ag nanowire.

To determine the spectral behavior of the light scattering properties, we have also performed extensive spectral studies in the darkfield light scattering. Figure 6 shows darkfield scattering spectra from Ag and Au wire and compare them to light scattering (Mie) theory. Figure 6(a) and (c) show the measured lightscattering spectra from the Ag and Au wires respectively. The good agreement with Mie theory presented in figures 6(b)

and (d), enabled us to start systematic investigations of the light scattering from wires of different diameter and length.

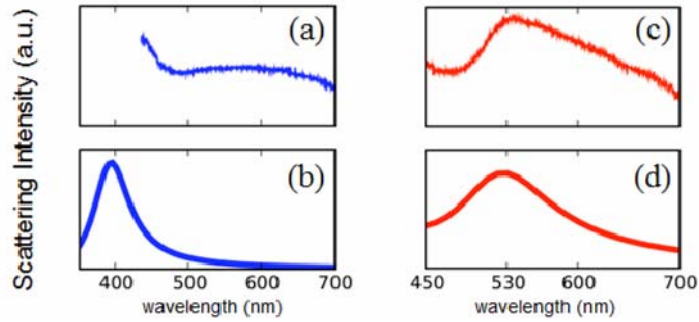


**Figure 6:** Measured (a and c) and simulated lightscattering spectra (b and d) from Au and Ag wires.

We have also synthesized 10 nm diameter Ag nanoparticles with 3nm thick SiO<sub>2</sub> coatings in solution. These particles were incorporated into organic thin films and their effect on the luminescence and optical absorption was analyzed. We found that, despite the 3 nm thick SiO<sub>2</sub> coating, the Ag nanoparticles still had a strong effect on the optical absorption, as shown in Fig. 7(a). Moreover, we note that the absorption enhancement is broadband. This makes such particles useful in enhancing the conversion efficiency of photovoltaic cells. Finally, we found that, because of the SiO<sub>2</sub> coating, the Ag nanoparticles have no deleterious effect on the luminescence, as shown in Fig. 7(b). This is a major step forward in producing solar cells that use metal nanostructures to enhance photocurrent through photonic effects while not impeding device operation through excitation quenching.

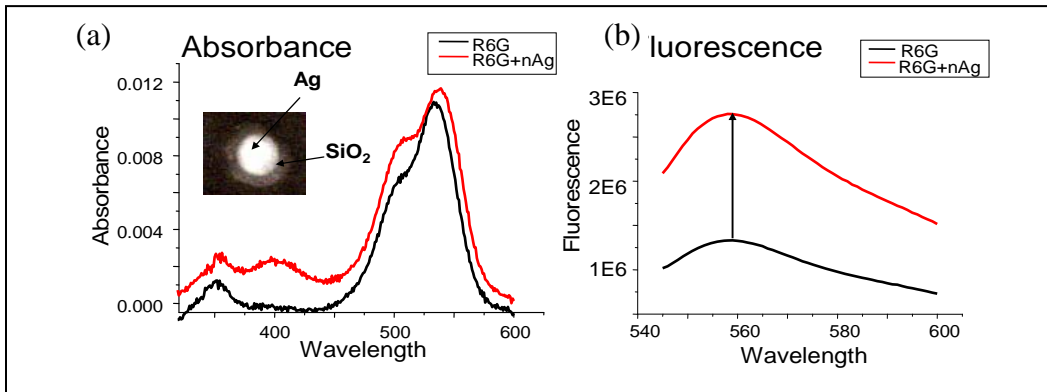


**Figure 7:** a) Effect of Ag-core (10 nm)/SiO<sub>2</sub> shell (3 nm) nanoparticles embedded in an organic thin film in the absorbance (a) and photoluminescence (b). Both absorbance and photoluminescence are enhanced by the presence of the Ag-core/SiO<sub>2</sub>-shell nanoparticles.

We have also explored the effect of the metal nanoparticle shape on the absorption and fluorescence enhancement. Figure 8 shows a transmission electron micrograph of Au nanoparticles of various shapes synthesized in solution. Furthermore, these nanoparticles have been incorporated into organic thin films using our newly developed aerosol

deposition process, yielding, for the first time, precisely controlled multilayer organic-metal nanostructures.

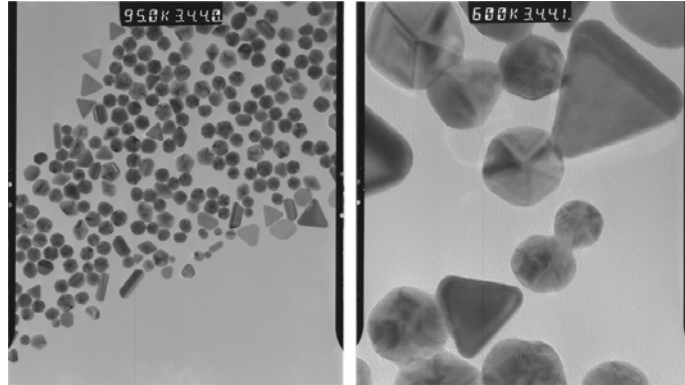


**Figure 8.** Transmission electron micrograph of solution synthesized Au nanocrystals. The average particle diameter is 10nm.

As the third major research direction in our team effort, we aimed to include the solution-synthesized metal nanoparticles into an organic solar cell without exposing the organic materials to solvents. The basic method was developed earlier under Peumans' Molecular Solar Cells GCEP grant for the inclusion of inorganic structures into organic solar cells. This method was then applied to include gold nanoparticles and nanorods at the active interface of simple bilayer organic solar cells, leading to an enhancement of their efficiency.

The physical mechanism behind the enhancement is a local concentration of the optical electric field, as shown in Fig. 9.

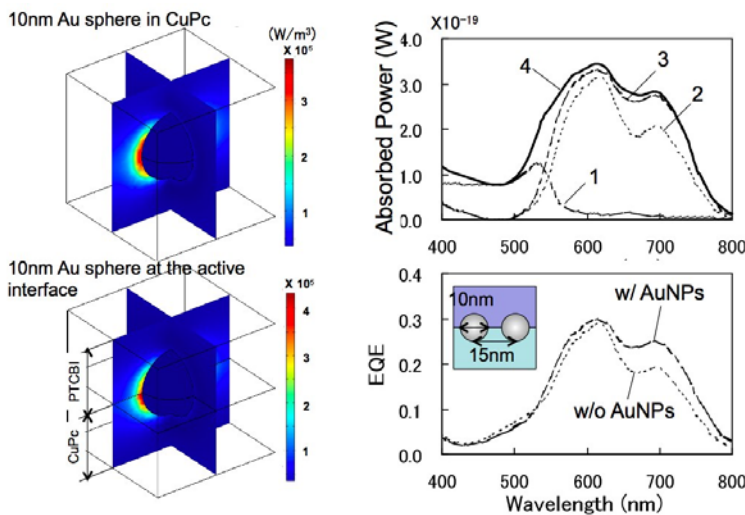


**Figure 8:** The presence of a 10 nm-diameter gold nanosphere in an organic matrix leads to increased optical absorption (top) and increased device performance (bottom) according to finite-element simulations.

Our experimental results agree with the simulation results of Fig. 9, with an increase in photocurrent by 20% to 30%, as shown in Fig. 10. As far as we know, this is the first demonstration of the use of metal nanoparticles to enhance the performance of organic solar cells using near-field effects.

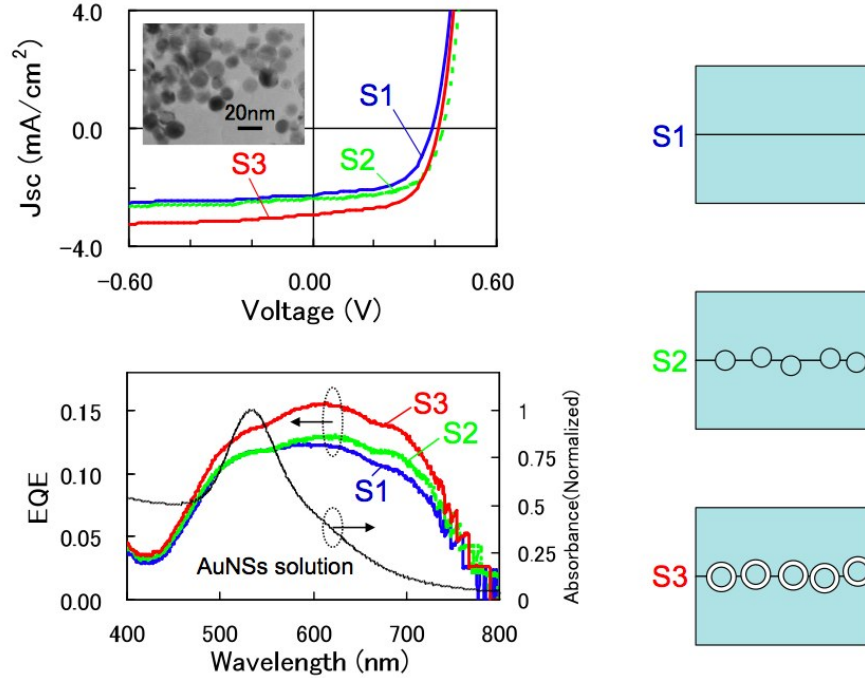


**Figure 10:** (Top) Increase in photocurrent for a bilayer cell when metal nanoparticles are included at the interface between the donor and acceptor of a simple bilayer organic solar cell. S1 is a control device without metal nanoparticles, S2 is a device with metal nanoparticles coated with an alkanethiol and S3 is a device in which a thin wide-bandgap coating was used to further electrically isolate the nanoparticles from the organic matrix. (Bottom) Increase in external quantum efficiency.

In order to further optimize the light concentration ability of metallic nanostructures we have derived inspiration from microwave antenna structures. Such structures enable a very strong light-matter interaction when the metal antenna length equals half the free space wavelength ( $\lambda_0/2$ ). Due to the difference in the optical behavior in the microwave and visible frequency regimes, we found that nanoscale metallic antennas need to be a substantially shorter than half the free space wavelength of light. In the visible regime, we found that metallic rods act as tiny Fabry-Perot cavities for (short range) surface plasmon-polariton waves that bounce back and forth between the antenna ends. For this reason, maximum field enhancements can be attained when the metallic antennas are approximately half of the surface plasmon-polariton wavelength ( $\lambda_{SPP}/2$ ). This effect is seen in Figure 11, which shows the calculated field intensity enhancements at the ends of 50 nm thick metallic strip antennas for different illumination wavelengths and antenna lengths.

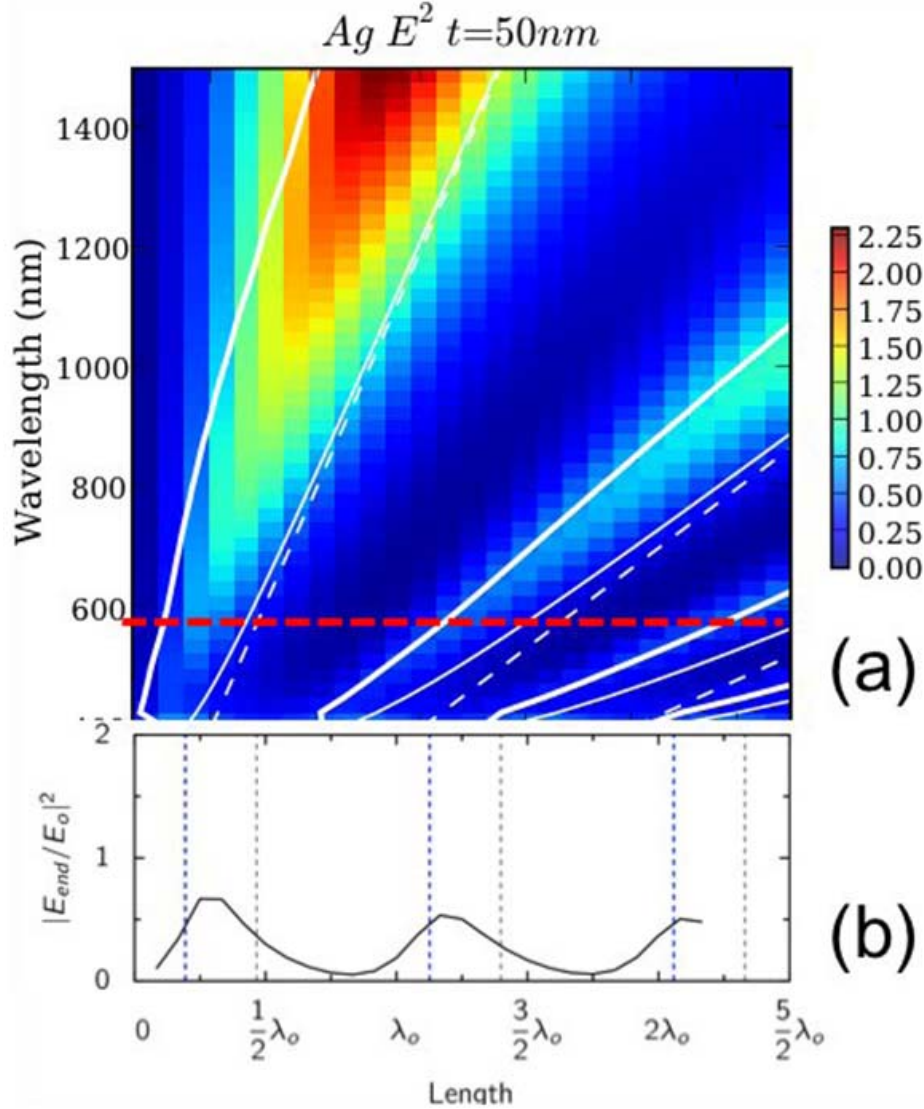


**Figure 11:** (a) Field intensity enhancements at the terminal ends of a metallic stripe antenna as a function of the antenna length and the illumination wavelength. (b) A cross-section of the field intensities at a wavelength of 580 nm. High field intensities are attained when the length of the antenna is close to  $0.5(n+1)\lambda_{spp}$ , where  $\lambda_{spp}$  is the surface plasmon-polariton wavelength and  $n$  is an integer. Note that resonances occur at significantly shorter antenna lengths than is the case for microwave antennas, which would resonate at  $0.5(n+1)\lambda_0$ , where  $\lambda_0$  is the free space wavelength.

Finally, we have used a very general theoretical framework to determine the maximum optical absorption in a limited volume of absorber; Achieving the highest possible optical absorption for a given volume or thickness of an absorber is a general problem in solar cells. The amount of active material (absorber) used is minimized to either minimize cost (in crystalline Silicon) or to maximize the internal efficiency (all solar cells and organic solar cells in particular). Several approaches have been developed, such as textures, gratings (guided resonances), cavities, plasmonic approaches, optical antennas, etc.

We have derived a general limit to the effectiveness of light trapping using concepts borrowed from information theory (singular value decomposition). The limit is applicable to all optical structures, including dielectric and metallic (sometimes called plasmonics) nanostructures. Not surprisingly, the limit is identical to that derived earlier for the geometric optics regime. The limit is:

$$\eta = \frac{4n^2}{\sin^2 \theta}, \quad (2)$$

where  $n$  is the index of refraction,  $\theta$  is the acceptance angle and  $\eta$  is the enhancement in optical absorption.

We confirmed that this limit holds for a number of geometries using computational electromagnetics. As an example, the optical absorption of a 250nm-thin film of amorphous Si was optimized by optimally shaping the thin film, resulting in an optical absorption bound by the above limit. The results are shown in Fig. 12.

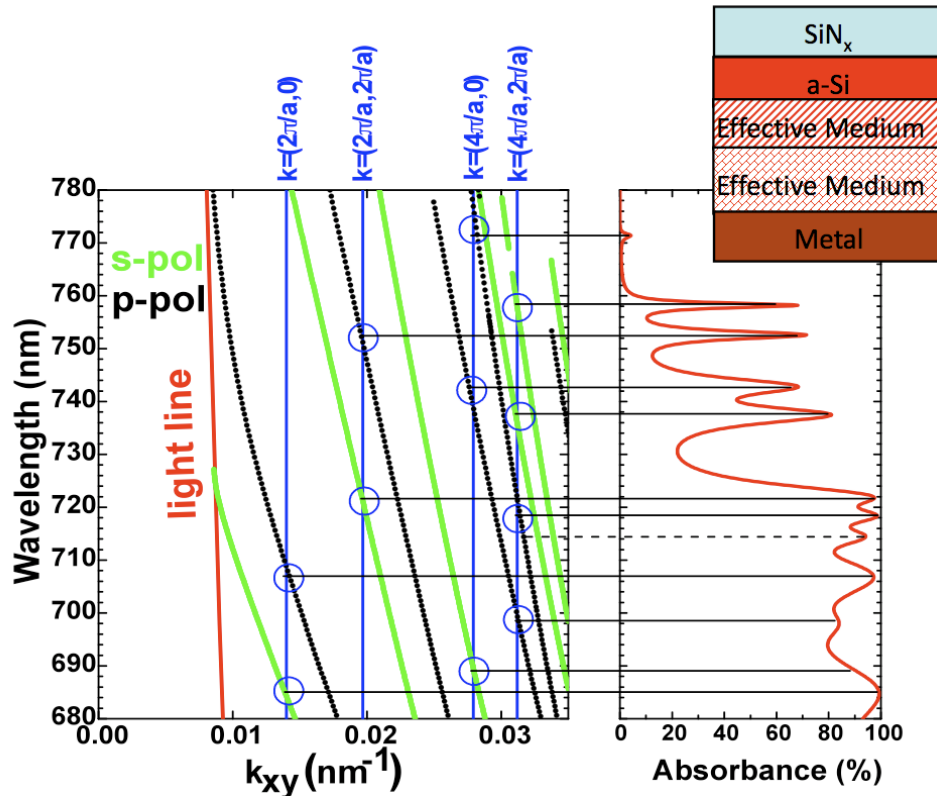


**Fig. 12.** Analysis of a thin-film amorphous Si 2D broadband grating light coupler. By structuring the film as a 2D grating, the optical absorption can be enhanced by a factor  $4n^2$ . This approach works by ensuring uniform coupling of incident light into the quasi-guided modes supported by the structure.

## Conclusions

Over the last three years, we have obtained very promising results in the development of transparent contacts, the design and synthesis of metallic nanoantennas, and the enhancement (upto 30%) of organic solar cells by incorporation of such plasmonic structures. We have taken plasmonics technology for application in organic solar cells to a new level and derived fundamental limits on the achievable performance enhancements. In our research we have witnessed an increase in solar performance through the incorporation of metallic nanostructures using scalable technologies. As a result, OPV offers an increased competitiveness for clean energy production compared to routes that ultimately lead to green house gas emissions. In order to have a global impact, methods for efficient scaling of this technology will have to be explored further in the future.

## Publications

1. P. B. Catrysse and S. Fan, "Near-complete transmission through sub-wavelength hole arrays in phonon-polariton thin films", *Physical Review B* 75, 075422 (2007).
2. P. B. Catrysse and S. Fan, Enlarging the bandwidth of nanoscale propagating plasmonic modes in deep sub-wavelength cylindrical holes, *Appl. Phys. Lett.* 91:18, 181118 (2007).
3. P. B. Catrysse and S. Fan, Propagating plasmonic modes and its implications for extraordinary transmission, *J. Nanophotonics* 2, 021790 (2008). (Invited paper)
4. S. Fujimori, R. Dinyari, J.-Y. Lee and P. Peumans, "Plasmonic light concentration in organic solar cells," accepted in *Nanoletters*.
5. S. Fujimori, R. Dinyari and P. Peumans, "Electrically-assisted aerosol deposition of metal nanoparticles," in preparation.
6. "Spectral Properties of Plasmonic Resonator Antennas," Edward S. Barnard, Justin S. White, Anu Chandran, and Mark L. Brongersma, *Opt. Express*, 16, 16529-16537 (2008).
7. P. B. Catrysse and S. Fan, Connecting the dispersion of the coaxial plasmonic structure and the planar metal-insulator-metal geomtry, *Appl. Phys. Lett* (submitted)
8. J.-Y. Lee and P. Peumans, "The origin of enhanced optical absorption in plasmonic solar cells with spherical metal nanoparticles," submitted.
9. M. Agrawal and P. Peumans, "The limits to light trapping in the sub-wavelength optical domain," submitted.
10. M. Agrawal and P. Peumans, "A very efficient light harvesting scheme for thin-film photovoltaics," submitted.

## Contacts

Brongermsa@stanford.edu, Ppeumans@stanford.edu, Shanhui@stanford.edu